### **Research Article**

# A Hyperspectral Imaging Tympanoscope as a Diagnostic Tool: System Development and a Pilot Study

Tayebe Taghizade<sup>1</sup>, Saeid Farahani<sup>1\*</sup>, Ali Kouhi<sup>2,3</sup>, Ali Balooch<sup>4</sup>, Alireza Akbarzade-Baghban<sup>5,6</sup>, Mohammad Esmaili<sup>7</sup>

- 1. Department of Audiology, School of Rehabilitation, Tehran University of Medical Sciences, Tehran, Iran
- <sup>2</sup> Department of Otolaryngology Head and Neck Surgery, Amir A'lam Hospital, Tehran University of Medical Sciences, Tehran, Iran
- <sup>3.</sup> Otorhinolaryngology Research Center, Tehran University of Medical Sciences, Tehran, Iran
- <sup>4</sup> Noorimentajhiz Company, Science and Technology Park, Kashan, Iran
- <sup>5</sup> Proteomics Research Center, Shahid Beheshti University of Medical Sciences, Tehran, Iran
- 6. Department of Biostatistics, School of Allied Medical Sciences, Shahid Beheshti University of Medical Sciences, Tehran, Iran
- <sup>7</sup> Municipality Organization, Qom, Iran

#### **ORCID ID:**

Tayebe Taghizade: 0009-0003-2720-5022 Saeid Farahani: 0000-0003-2541-283X Ali Kouhi: 0000-0002-4154-8908 Ali Balooch: 0009-0000-5239-7175

Alireza Akbarzade-Baghban: 0000-0002-0961-1874

Mohammad Esmaili: 0009-0006-3419-1492

**Citation:** Taghizade T, Farahani S, Kouhi A, Balooch A, Akbarzade-Baghban A, Esmaili M. A Hyperspectral Imaging Tympanoscope as a Diagnostic Tool: System Development and a Pilot Study. Aud Vestib Res. 2026;35(1):?-?.

### **Article info:**

Received: 24 Apr 2025 Revised: 19 Jul 2025 Accepted: 02 Aug 2025

\* Corresponding Author: Department of Audiology, School of Rehabilitation, Tehran University of Medical Sciences, Tehran, Iran. s\_farahani@tums.ac.ir

**Short running title:** A Hyperspectral Imaging Tympanoscope as a...

# **Highlights:**

- Diagnosis of MEE is a challenging task due to the lack of reliable diagnostic tools
- The hyperspectral tympanoscope is a cost-effective imaging method for detecting MEE
- NIR imaging can distinguish between the presence or absence of fluid in the ME

### **ABSTRACT**

**Background and Aim:** Accurate diagnosis of Middle Ear Effusion (MEE) is a challenging task due to the lack of reliable diagnostic tools available to physicians and audiologists. This study aimed to develop a hyperspectral imaging tympanoscope for diagnosing MEE and evaluate its diagnostic ability.

**Methods:** The tympanoscope system was constructed using an ear endoscope, lens, camera, and near-infrared wavelengths. Its diagnostic ability was evaluated with a middle ear-mimicking phantom. Additionally, a pilot study was conducted on middle ear images from 10 children (five healthy and five with MEE).

**Results:** Phantom experiments revealed a Weber contrast difference of 0.16 and 0.49 between phantoms with and without fluid in visible otoscopy and hyperspectral tympanoscopy, respectively. As a result, in hyperspectral tympanoscopy, the contrast difference between fluid presence and absence was nearly tripled. Furthermore, in the pilot study, a significant difference was found in Weber contrast between healthy children and those with MEE (p<0.001), with higher contrast in the MEE group.

**Conclusion:** The hyperspectral imaging tympanoscope can quantitatively distinguish between the presence or absence of fluid in the middle ear. It has potential as a diagnostic and monitoring tool for MEE.

**Keywords:** Hyperspectral; tympanoscope; middle ear effusion; middle ear-mimicking phantom

#### Introduction

Middle Ear Effusion (MEE), characterized by fluid accumulation in the middle ear cavity, often results from Tympanic Membrane (TM) infection [1-3]. It is the second most common disease diagnosed in children after acute upper respiratory tract infections, with at least 80% experiencing one or more episodes by age 3 [4, 5]. Diagnosis primarily relies on otoscopy or endoscopy using a white light source to assess TM color changes and mobility [6, 7]. However, precise diagnosis is challenging due to overlapping symptoms, such as inflammation and temporary hearing loss, leading to significant dependence on the examiner's expertise [8]. Diagnostic instruments include the otoscope, video otoscope, pneumatic otoscope, tympanometry, acoustic reflex measurement and broadband tympanometry [9]. The conventional tests are subjective, with interpretation varying widely among physicians [6]. In a study, the error rate in diagnosing middle ear diseases using digital imaging with a traditional otoscope was reported 50% for pediatricians and 27% for otolaryngologists [7]. Another study estimated the accuracy of otitis media diagnosis by pediatricians at 51%, resulting in overdiagnosis (false positives) in 26% of cases [4, 9, 10]. Conversely, MEE is often underestimated (false negatives) due to its asymptomatic nature and the limitations of conventional otoscopy [10]. Therefore, there is a need for tools providing additional objective insights to improve diagnostic accuracy [7].

Hyperspectral imaging has demonstrated enhanced information for accurate disease detection compared to standard imaging [7, 11-17]. Near-Infrared (NIR) wavelengths experience minimal attenuation at the TM, enabling greater light transmission and improved visualization of structures behind it. Kashani et al. developed a Shortwave Infrared (SWIR) otoscope for imaging middle ear structures and fluid within the SWIR region, predicting effusion presence with over 90% specificity and sensitivity [18]. It should be noted that attenuation decreases considerably in the infrared and SWIR ranges, but imaging at these wavelengths requires specialized optics and photon detectors, substantially increasing device cost [8, 9]. Rajamanickam used a visual NIR hyperspectral otoscope (600–1050 nm) for high-sensitivity fluid detection and precise diagnosis of middle ear infections, demonstrating peak contrast between ossicles and fluid at 1000 nm in a phantom model [9]. Most observations to date have concentrated on the visible wavelength range (400–700 nm), similar to conventional white light otoscopy [7]. In this study, we propose a hyperspectral imaging tympanoscope for visualizing MEE and comparing healthy and infected states. The goal is to determine an appropriate NIR wavelength capable of detecting MEE with high sensitivity. It can provide physicians and audiologists with an objective, quantitative method to detect MEE presence, a condition currently diagnosed subjectively, focusing on system design and preliminary evaluation in a small sample.

### Methods

# Tympanoscope design

A hyperspectral imaging tympanoscope was developed using an ear endoscope. Endoscopes vary in tube length, diameter, and viewing angle (0–30 degrees). We employed a 4-mm diameter, 10-cm length endoscope with a zero-degree angle for direct insertion into the ear canal. An integrated lens provides a clear display image with the power source located at the base. Although white light is standard, we used Light-Emitting Diodes (LEDs) emitting specific wavelengths. A Closed-Circuit Television (CCTV) lens (25-mm focal length) was positioned between the endoscope lens and the camera to project the eardrum image onto the camera detector. The camera, with a Sony IMX179 CCD sensor (3288×2512 resolution, 8-bit depth, frame rate up to 30 fps), captured the

images. Figure 1A illustrates the schematic image of the tympanoscope, and Figure 1 B shows the 3 D image of this device. The body, designed in SolidWorks using 7000-series aluminum alloy, had all the required components.

Based on a pilot study and previous data [7, 9, 18], wavelengths of 640 nm and 940 nm were initially selected for middle ear monitoring. The 940-nm wavelength was selected because TM transparency increases at longer wavelengths compared to visible light, revealing details behind the TM more clearly [9, 18]. Since silicon-based camera sensitivity extends to approximately 1000 nm, a 940-nm wavelength was suitable. This wavelength can pass through the TM, reflect off structures behind it, and aid effusion detection. The 640-nm visible wavelength was used for comparison with NIR images in the phantom model.

A LabVIEW code processed raw data from the tympanoscope and reconstructed images at the specified wavelength, saving them as JPEG files. Figure 2 shows the user interface of this software, which allows setting the gain and exposure time of images. Using the digital tympanoscope, the TM position was visualized and adjusted before image capturing. The software recorded and saved TM images on the monitor.

# Pilot study for functionality evaluation

The device's functionality was assessed by participating 10 children (aged 3–12): five healthy controls (mean age: 6.2 years) and five diagnosed with unilateral MEE (mean age: 6.4 years). This sample size is appropriate for a feasibility study, as similarly employed by Cavalcanti et al. [8] to assess early-stage device potential. MEE presence was verified through tympanometry and evaluation by two physicians. Any cerumen was removed. Procedures were explained to all participants, and informed consent was obtained. An expert audiologist fixed the child's head in a sitting position and captured NIR TM images using the developed hyperspectral tympanoscope. The endoscope was inserted until a clear closed TM image appeared on the monitor, standardizing the camera-to-TM distance across participants despite varying canal lengths.

Image contrast, indicating pixel intensity variation across image regions, is crucial for NIR imaging [9], which relies on differences between middle ear structures (e.g., ossicles, fluid). Weber contrast was measured at 940 nm for normal and infected ears, using the following formula:  $(I_{max}-I_{min})/I_{min}$ , where  $I_{max}$  represents malleus intensity and  $I_{min}$  is the background intensity [9]. To determine the Weber contrast, the intensity of the light reflected from the ossicle and air/effusion was recorded by creating a small box on different areas of the TM using image processing software, as shown in Figure 3. The box determination was in accordance with the research conducted by Carr et al. [5]. Intensity normalization was used to maximize the intensity difference between different areas. For this purpose, the software set the pixel of the image as follows: highest intensity=255, lowest intensity=0. In this way, all image pixels were normalized based on intensity. Figure 3 depicts NIR images of the normal middle ear (Figure 3 A) and the middle ear with effusion (Figure 3 B). TM regions were marked as: green (normal TM), red (TM with effusion), or blue (malleus).

The independent t-test was used to compare the Weber contrast between groups. Normality of data distribution was assessed using the Shapiro-Wilk test, and equality of variances was evaluated using Levene's test. All statistical analysis was performed in SPSS v.26. The Shapiro-Wilk test confirmed normal data distribution in both groups (p>0.05). Levene's test showed no significant variance difference (p>0.05).

## Diagnostic evaluation using a middle ear-mimicking phantom

A phantom replicating the ear canal, TM, malleus, and middle ear cavity assessed the device's ability to detect and distinguish fluids behind a semitransparent membrane. The phantom was designed with SolidWorks software and manufactured using a 3D printer (Jahan 3D). It featured a 2-mL cubic cavity approximating human middle ear capacity. A latex medical glove rubber film ( $\Box 0.18$  mm thick) was used, simulating TM properties [8]. Figure 4 details this ear-mimicking phantom, including the schematic model (Figure 4 A) and the printed model utilized in our study (Figure 4 B). The phantom was designed with two openings; a stretched latex sheet was secured to the front window, and the manubrium was placed behind it. A cylinder (12 mm diameter, 25 mm length) coupled to this window simulated the ear canal. A second window facilitates the introduction of effusion-mimicking fluids into the middle ear model. Orange juice was selected for its optical similarity to MEE, as demonstrated in previous studies [5], although we acknowledge that it does not fully replicate the properties of real effusion. In addition, an empty phantom simulated a healthy middle ear. Images of empty and fluid-filled phantoms were captured at 640-nm and 940-nm wavelengths for evaluation.

#### **Results**

# **Functionality evaluation**

The NIR imaging tympanoscope captured high-resolution images of MEE at 940 nm. Comparing images from 10 children (five controls, five with MEE) revealed that the effusion visualized by the hyperspectral imaging tympanoscope was typically undetectable due to limited visible light transmission through the TM.

Figure 5 displays Weber contrast values for NIR images in controls and MEE cases. According to Schmilovitch et al., reflectance is lower from a TM affected by MEE, resulting in reduced intensities [19]. Consequently, effusion presence significantly increased the mean Weber contrast from  $0.28\pm0.02$  to  $0.56\pm0.04$ . The independent t-test results revealed a significant difference in Weber contrast between healthy children and those with MEE (t=10.97, p<0.001, 95% CI: 0.21-0.32), with a higher contrast in the MEE group. Furthermore, the effect size (Cohen's d=6.94) indicated a huge practical significance. The large effect size is likely due to the small sample size and the selection of quite distinct samples in two groups and intensity normalization; thus, further validation in larger studies is needed.

# **Diagnostic evaluation**

The 3D-printed phantom assessed fluid detection performance. Distinguishing empty and fluid-filled states under visible light was challenging, highlighting the difficulty of fluid detection with traditional otoscopy [9]. Therefore, NIR wavelengths were anticipated to provide superior optical contrast compared to visible imaging for detecting middle ear fluid. The Weber contrast obtained from the phantom image under visible light for empty and fluid-filled states was 0.18 and 0.34, respectively. Also, the Weber contrast obtained from the phantom image under NIR light for empty and fluid-filled states was 0.16 and 0.65, respectively. As shown in Figure 6, the Weber contrast difference between phantoms with and without fluid in visible otoscopy and hyperspectral imaging tympanoscopy was 0.16 and 0.49, respectively. Thus, the contrast difference between empty and fluid-filled states was nearly tripled under NIR imaging. This enhanced contrast significantly aids physicians in detecting middle ear fluid.

### **Discussion**

The hyperspectral imaging tympanoscope designed in our study offers a promising, cost-effective solution for detecting MEE. We demonstrated high-sensitivity fluid detection in phantom models. While otoscopy remains the primary method for MEE detection, conventional visible light otoscopy has limited accuracy, with correct diagnosis rates of 46% for general practitioners, 51% for pediatricians, and 76% for otolaryngologists [5]. Previous research confirms reduced light attenuation at longer wavelengths [5]. Improved NIR transmission benefits otoscopy, as the light must penetrate the TM after reflecting off middle ear structures like the highly reflective ossicles and promontory before reaching the detector. Absorption or scattering by the TM reduces light reaching middle ear structures and further diminishes the reflected signal intensity returning to the detector, degrading image contrast and resolution. The hyperspectral imaging approach depends on the contrast between different regions of the middle ear, such as the ossicles and fluid. For middle ear structures visible conventionally, the hyperspectral tympanoscope enhances contrast [9]. The hyperspectral imaging tympanoscope can differentiate between fluid-filled and empty middle ear regions. The generated NIR contrast can help clinicians in determining fluid presence. Overall, reflectance in fluid-filled areas is greater in the visible range and gradually decreases as the spectrum shifts toward the NIR region. NIR wavelengths exhibit minimal TM attenuation and greater transmission, improving visualization of structures behind the TM [8].

Kashani et al. constructed a SWIR otoscope for imaging the middle ear structures and fluid in 30 children undergoing tympanostomy tube surgery in the SWIR region. Their results showed that SWIR light creates better contrast between fluid-filled and air-filled spaces than visible light [18]. While attenuation decreases further in SWIR/infrared regions, imaging requires specialized optics and photon detectors that are costly [9, 18]. Therefore, this study utilized the NIR range to develop a cost-effective, highly sensitive hyperspectral imaging tympanoscope for MEE detection. Our phantom results showed a greater contrast difference between fluid presence and absence under NIR imaging compared to visible otoscopy. Furthermore, the pilot study on humans suggested hyperspectral tympanoscopy can detect MEE based on strong fluid absorption around 940 nm, yielding higher contrast in MEE images than in normal ear images.

This study reported the hyperspectral tympanoscope's potential as a novel diagnostic imaging method for detecting MEE. Applying NIR light extends the usable spectrum to wavelengths where middle ear fluid contrast is significantly higher than in the visible range, enabling a more objective assessment of MEE presence. Objectifying this historically inconsistent diagnosis could minimize overprescription of antibiotics and reduce unnecessary tympanostomy tube surgeries, among the most common pediatric procedures. However, the current findings are limited to system design and preliminary evaluation by inclusion of a small sample size; comprehensive clinical validation using a larger sample size will be reported in the future. In our future study, the sensitivity, specificity, false positive and negative rates, predictive values, likelihood ratios, and kappa agreement coefficients will be evaluated. Additionally, artificial intelligence algorithms will be developed to enable automated detection of middle ear effusion.

#### **Conclusion**

The designed hyperspectral imaging tympanoscope is able to distinguish fluid-filled and empty middle ears. It is also suitable for diagnosing Middle Ear Effusion (MEE) in children. However, to confirm these findings, further clinical studies with a larger sample size involving patients with conditions like acute otitis media and MEE are needed. This system offers a cost-effective diagnostic solution for middle ear diseases in developing countries. Further studies are recommended to integrate hyperspectral tympanoscopy with artificial intelligence algorithms, which can lead to automated diagnosis of MEE and can be used as a screening technique in settings where there are not enough specialists.

### **Ethical Considerations**

# **Compliance with ethical guidelines**

The experimental protocol was approved by the Ethical Committee of Tehran University of Medical Sciences with the document no. IR.TUMS.FNM.REC.1402.211.

# **Funding**

This study was conducted under grant No.1403-2-103-72924 approved by Tehran University of Medical Sciences.

### **Authors' contributions**

TT: Conceptualization, design of the study, data collection, interpretation of the results, drafting the manuscript; SF: Conceptualization, interpretation of data and revision of the manuscript; AK: Conceptualization and editing; AB: Conceptualization, design and manufacture of the device; AAB: Statistical analysis; ME: Conceptualization, design and manufacture of the device.

### **Conflict of interest**

The authors declare that there is no conflict of interest regarding the publication of this paper.

# Acknowledgments

We would like to thank the parents of the study community for their participation and the success of this project. We also thank the children who participated in the study.

### References

- 1. Lieberthal AS, Carroll AE, Chonmaitree T, Ganiats TG, Hoberman A, Jackson MA, et al. The diagnosis and management of acute otitis media. Pediatrics. 2013;131(3):e964-99. [DOI:10.1542/peds.2012-3488]
- 2. Qureishi A, Lee Y, Belfield K, Birchall JP, Daniel M. Update on otitis media prevention and treatment. Infect Drug Resist. 2014;7:15-24. [DOI:10.2147/IDR.S39637]
- 3. Sundvall PD, Papachristodoulou CE, Nordeman L. Diagnostic methods for acute otitis media in 1 to 12 year old children: a cross sectional study in primary health care. BMC Fam Pract. 2019;20(1):127. [DOI:10.1186/s12875-019-1018-4]
- 4. Abbott P, Rosenkranz S, Hu W, Gunasekera H, Reath J. The effect and acceptability of tympanometry and pneumatic otoscopy in general practitioner diagnosis and management of childhood ear disease. BMC Fam Pract. 2014;15:181. [DOI:10.1186/s12875-014-0181-x]
- 5. Carr JA, Valdez TA, Bruns OT, Bawendi MG. Using the shortwave infrared to image middle ear pathologies. Proc Natl Acad Sci U S A. 2016;113(36):9989-94. [DOI:10.1073/pnas.1610529113]
- 6. Valdez TA, Pandey R, Spegazzini N, Longo K, Roehm C, Dasari RR, et al. Multiwavelength fluorescence otoscope for video-rate chemical imaging of middle ear pathology. Anal Chem. 2014;86(20):10454-60. [DOI:10.1021/ac5030232]
- 7. Tran Van T, Lu Thi Thao M, Bui Mai Quynh L, Phan Ngoc Khuong C, Huynh Quang L. Application of Multispectral Imaging in the Human Tympanic Membrane. J Healthc Eng. 2020;2020:6219845. [DOI:10.1155/2020/6219845]

- 8. Cavalcanti TC, Kim S, Lee K, Lee SY, Park MK, Hwang JY. Smartphone-based spectral imaging otoscope: System development and preliminary study for evaluation of its potential as a mobile diagnostic tool. J Biophotonics. 2020;13(6):e2452. [DOI:10.1002/jbio.201960213]
- 9. Rajamanickam GP. A multispectral imaging method and device to detect and quantify the presence of fluid in the middle ear to facilitate the diagnosis and triage of ear infections. [Dissertation]. Cambridge, MA: Massachusetts Institute of Technology; 2020.
- 10. Rosenfeld RM. Diagnostic certainty for acute otitis media. Int J Pediatr Otorhinolaryngol. 2002;64(2):89-95. [DOI:10.1016/s0165-5876(02)00073-3]
- 11. Valdez TA, Carr JA, Kavanagh KR, Schwartz M, Blake D, Bruns O, et al. Initial findings of shortwave infrared otoscopy in a pediatric population. Int J Pediatr Otorhinolaryngol. 2018;114:15-9. [DOI:10.1016/j.ijporl.2018.08.024]
- 12. Valdez TA, Spegazzini N, Pandey R, Longo K, Grindle C, Peterson D, et al. Multi-color reflectance imaging of middle ear pathology in vivo. Anal Bioanal Chem. 2015;407(12):3277-83. [DOI:1s00216-015-8580-y]
- 13. Kapsokalyvas D, Bruscino N, Alfieri D, de Giorgi V, Cannarozzo G, Cicchi R, et al. Spectral morphological analysis of skin lesions with a polarization multispectral dermoscope. Opt Express. 2013;21(4):4826-40. [DOI:10.1364/OE.21.004826]
- 14. Bae SJ, Lee DS, Berezin V, Kang U, Lee KH. Multispectral autofluorescence imaging for detection of cervical lesions: A preclinical study. J Obstet Gynaecol Res. 2016;42(12):1846-53. [DOI:10.1111/jog.13101]
- 15. Spigulis J, Oshina I, Berzina A, Bykov A. Smartphone snapshot mapping of skin chromophores under triple-wavelength laser illumination. J Biomed Opt. 2017;22(9):91508. [DOI:10.1117/1.JBO.22.9.091508]
- 16. Rey-Barroso L, Burgos-Fernández FJ, Delpueyo X, Ares M, Royo S, Malvehy J, et al. Visible and Extended Near-Infrared Multispectral Imaging for Skin Cancer Diagnosis. Sensors (Basel). 2018;18(5):1441. [DOI:10.3390/s18051441]
- 17. Ortega S, Fabelo H, Iakovidis DK, Koulaouzidis A, Callico GM. Use of Hyperspectral/Multispectral Imaging in Gastroenterology. Shedding Some Different Light into the Dark, J Clin Med. 2019;8(1):36. [DOI:10.3390/jcm8010036]
- 18. Kashani RG, Młyńczak MC, Zarabanda D, Solis-Pazmino P, Huland DM, Ahmad IN, et al. Shortwave infrared otoscopy for diagnosis of middle ear effusions: a machine-learning-based approach. Sci Rep. 2021;11(1):12509. [DOI:10.1038/s41598-021-91736-9]
- 19. Schmilovitch Z, Alchanatis V, Shachar M, Holdstein Y. Spectrophotometric Otoscope: A New Tool in the Diagnosis of Otitis Media. J Near Infrared Spectrosc. 2007;15(4):209-15. [DOI:10.1255/jnirs.739]

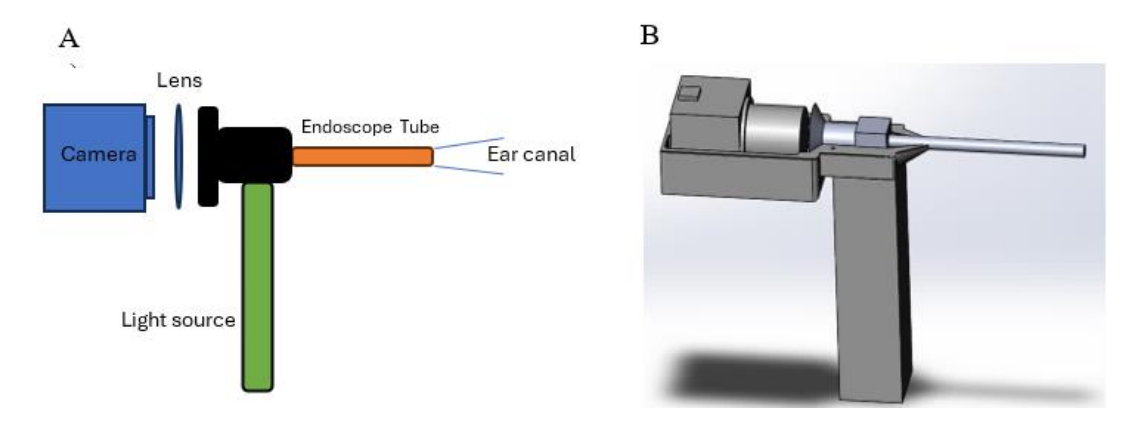


Figure 1. Hyperspectral tympanoscope. A) The schematic image of different components of the hyperspectral tympanoscope. B) The 3D image of the final hyperspectral tympanoscope

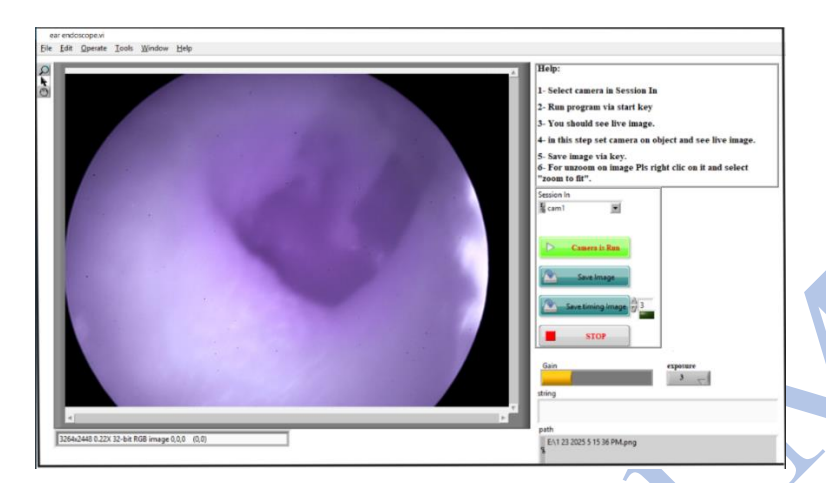


Figure 2. Screenshot of the developed lab view software

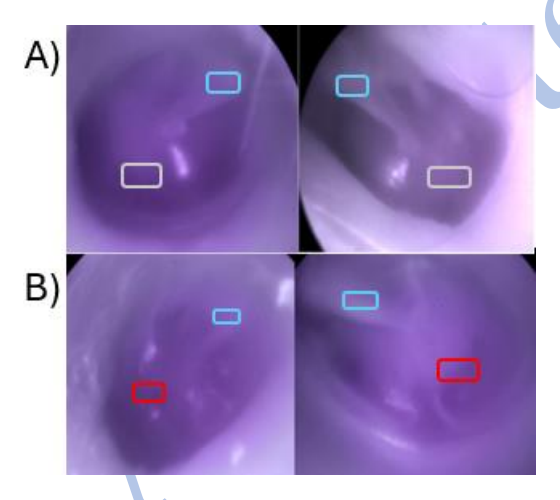


Figure 3. Near-infrared images of normal and abnormal human middle ears. A) Near-infrared images of two normal tympanic membranes. B) Near-infrared images of two ears with middle ear effusion

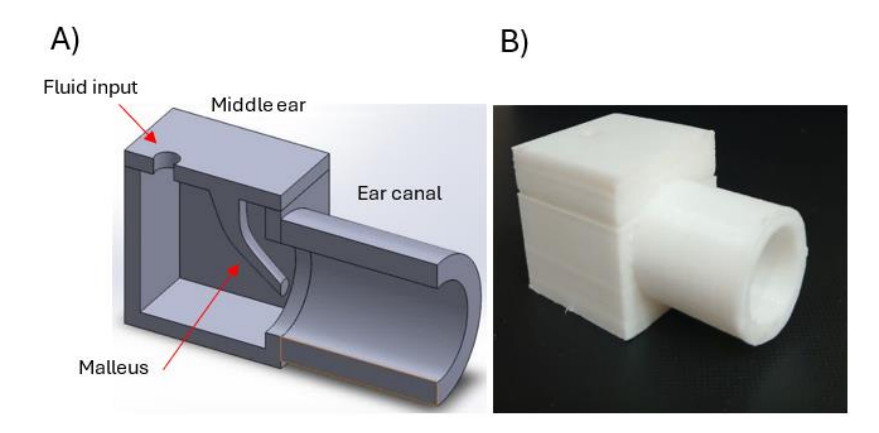


Figure 4. Middle ear-mimicking phantom; A) 3D model and B) printed and used in this study

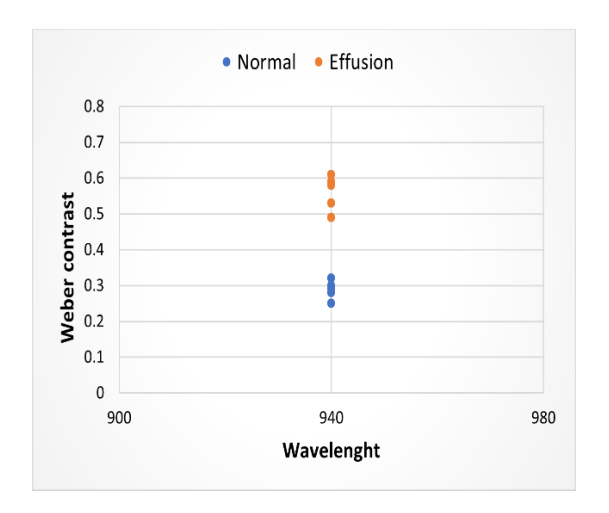


Figure 5. The Weber contrast values for near-infrared images in five normal children and five children with middle ear effusion

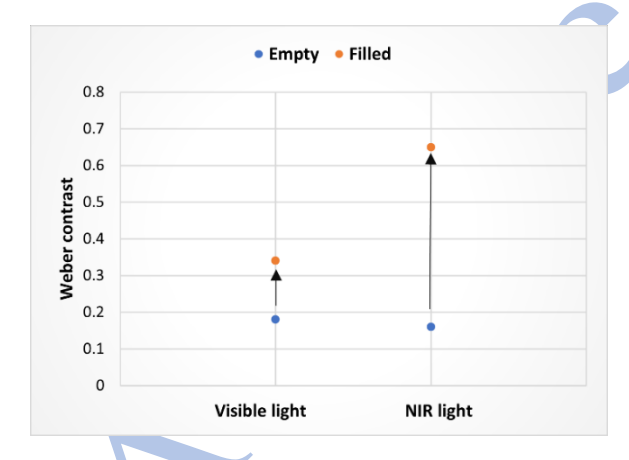


Figure 6. Weber contrast comparison between the empty and filled middle ear-mimicking phantoms with visible and Near-infrared imaging